IJNRD.ORG ISSN : 2456-4184
INTERNATIONAL JOURNAL OF NOVEL RESEARCH AND DEVELOPMENT (IJNRD) | IJNRD.ORG
An International Open Access, Peer-reviewed, Refereed Journal

Controlling Power Flow in a High-Voltage DC Link using an ANN and PI Controller

K. Sushma[1], Dr.K. Durga Syam Prasad[2], Mrs. K. Sravanthi[3]

[1] Pg Student, Dept. of Electrical and Electronics Engineering, Vignan's Institute of Engineering For Women, Visakhapatnam, A.P – 530049.

[2] Prof., Head of the Department, Dept. of Electrical and Electronics Engineering, Vignan's Institute of Engineering for Women, Visakhapatnam, A.P – 530049.

[3] Asst. Prof., Dept. of Electrical and Electronics Engineering, Vignan's Institute of Information Technology, Duvvada, Visakhapatnam. A.P

ABSTRACT

The purpose of this study to detail the modelling of a high-voltage direct-current (HVDC) system, that is used to transmit large amounts of electricity between 2 converter stations. Getting the power loss in the HVDC system down is the primary focus of this article. Power flow regulation is implemented to lessen these power losses. By manipulating the rectifier & inverter stations with an ANN, it is possible to regulate power flow. In this study, we present a simulation of a high-voltage direct-current (HVDC) system that relies on the CIGRE HVDC Benchmark. DC current Idref is measured on the inverter side, and the difference between this value and the observed DC current Id is the error signal e. An ANN controller is then utilised to transform this error into an alpha-order signal that is then used to regulate the width of the firing pulses applied to the converter's thyristors.

KEYWORDS: HVDC Transmission, Simulation, Artificial Neural Network, Conventional controller.

I. INTRODUCTION

The mercury arc valve was used in all of the earliest HVDC schemes. In 1972, the first back-to-back asynchronous interconnection took place along the Eel River between Quebec and New Brunswick, demonstrating the effectiveness of thyristor valves. Since then, thyristor valves have entirely phased out their mercury arc predecessors. More than a quarter of a million kilowatts (MW) of HVDC transmission capacity will have been built in over a hundred projects throughout the world by 2008, and another twelve-and-a-half million MW of HVDC transmission capacity will be planned for fifty projects5. Since DC transmission and technology are expanding at such a rapid rate, HVDC transmission should be a required course for incoming freshmen studying power systems. Most universities only offer one course in power systems at the undergraduate level, and that one is usually focused on alternating current transmission. York College of Pennsylvania offers a Bachelor of Science in Electrical and Computer Engineering with four different areas of emphasis: power systems/energy conversion, embedded systems, signal processing/communication, & control systems. HVDC transmission systems can be broken down into two distinct categories: those with two terminals, and those with multiple terminals, each with their own set of advantages and disadvantages in terms of operational needs, adaptability, and financial outlay. Submarine HVDC cables, such as the Konti-Skan, Fenno-Skan, Baltic cable, and Kontek HVDC links, often use a monopolar link with ground return. A monopolar link with metallic return (low insulation) may be utilised in place of a connection to the earth or the sea. Due to the lack of direct current passing via earth throughout operations, transformer magnetism saturation & electrochemistry corrosion can be avoided by using a monopolar link with a metallic return, despite the greater DC-line investment and operational expense associated with this configuration. At first, the Sweden-Poland The link was supposed to be a single-pole connection with a ground return.

An HVDC transmission system consists of three basic parts:

1) A rectifier station to convert AC to DC

2) A DC transmission line and
3) An inverter station to convert DC back to AC.

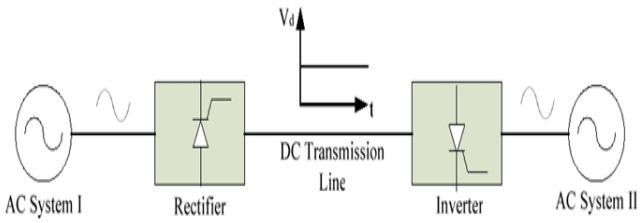

Figure 1. Schematic diagram of an HVDC transmission system

II. HVDC SYSTEM MODEL

High-performance numerical calculation, system simulation, & application development are all possible with MATLAB/SIMULINK. One of its design tools, Power System Blockset (PSB), is used for modelling and simulating electrical power systems in the SIMULINK environment. The electromagnetic and electromechanical equations form the basis of a block library containing typical components and equipment encountered in electrical power networks. Both power and control systems can be modelled and simulated with PSB/SIMULINK. By analysing the system's state variables, PSB can find solutions to the system's equations at a constant or varying integration time step. State-space equations in the discrete or continuous time-domain describe the system's linear dynamics. A selection of other integration algorithms is also available. HVDC system, as depicted in Fig. The system is a mono-polar 500 kilovolt (kV) 1000 megawatt (MW) HVDC connection with 12-pulse converters on both the rectifier and inverter sides, coupled to weak ac systems (short circuit ratio of 2.5 at rated frequency of 50 Hz) that present significant challenges for dc controls. On both ends, you will find filtering and reactive compensation systems that use capacitance. Specifically, the following subcircuits make up the power circuit of the converter.

A. AC Side

On either side of the converter are a supply network, filters, & transformers that make up the ac sides of HVDC system. Thevenin equivalent voltage source having equivalent source impedance stands in for the ac supply network. Harmonics from the converter are absorbed by the AC filters, and reactive power is supplied to the converter through the AC filters.

B. DC Side

Both the rectifier as well as the inverter sides of the converter use smoothing reactors on the dc side. An equivalent T network is used to represent the dc transmission line, which can be adjusted to the fundamental frequency to create a challenging resonant state for the modelled system.

C. Converter

To symbolise the converter stations, a 12-pulse arrangement is shown here, with two 6-pulse valves in series. Each valve in the real converter is made up of numerous thyristors connected in series. A parallel RC snubber is connected to each thyristor, so each valve does have a (di/dt) limiting inductor.

D. Power Circuit Modeling

Twelve-pulse converters, including the rectifier and inverter, are built from a pair of universal bridge blocks wired in series. Two grounded three-phase transformers, one with a Wye-Wye connection and the other with a Wye-Delta connection, represent the converter transformers. In a T-network configuration, the converters are linked together.

1) Universal Bridge Block:

The universal bridge block is an implementation of a global three-phase power converter using a bridge of six power switches. From this menu, you can choose the power switch & converter setup that best suits your needs. Each switch has an RC snubber circuit wired in parallel with it. All vector gating signals follow the natural order of commutation and consist of six pulse trains. In this model, and plenty measurements are not realised.

2) Three Phase Source:

The source is represented by a three-phase alternating current voltage source with an R-L combination in series.

3) Converter Transformer Model:

The three-phase, two-winding transformer types have been employed, with winding connection & winding parameters set using mask parameters. Tap position is set according to a multiplier applied to the converter transformers' principal nominal voltage (1.01 on rectifier side; 0.989 on inverter side). Saturation has been modelled to be reached. Saturation has been defined as a sequence of current/flux pairings (in p.u.), commencing with the pair (0,0).

III. CONTROL VARIABLES FOR CONSTANT POWER FLOW CONTROL

Measurements of (/) and the creation of firing pulses for the rectifier & inverter make up the bulk of the control model. To construct the firing signals, the PLO is employed. The PLO generates a ramp at its output that is timed to the phase. It's a commuting.

$$I_d = ((A_r * E_r / T_r) \cos \alpha_r - (A_i * E_i / T_i) \cos \gamma_i) / (R_{cr} + R_d - R_{ci}) \quad (3.1)$$

$$E_{dr} = (A_r * E_r / T_r) \cos \alpha_r \quad (3.2)$$

$$E_{di} = (A_i * E_i / T_i) \cos \gamma_i \quad (3.3)$$

Following are the controllers used in the control schemes:

1. Extinction Angle (γ) Controller
2. dc Current Controller;
3. Voltage Dependent Current Limiter (VDCOL).

1) Rectifier Control:

Constant Current Control (CCC) is utilised by the rectifier control system. The maximum allowable current is measured using the inverter as a reference. To protect the converter when the inverter side is lacking adequate dc voltage support (due to a defect) or load, this is done (load rejection). The dc voltage available on the inverter side is what determines the reference current utilised for rectifier control. An error signal is generated by comparing the measured and actual dc current on the rectifier side, which is accomplished by passing the measured and actual values via the appropriate transducers and filters. A PI controller is then used to generate the proper firing angle order based on the error signal. Using this data, the firing circuit employs the previously described technique to create equidistant pulses for the valves.

2) Inverter Control:

On the inverter side, we have created Extinction Angle Control, also known as control and current control. Here, PI controllers have been used to implement a CCC equipped with a Voltage Dependent Current Order Limiter (VDCOL). VDCOL (implemented via lookup table) output is compared to an external reference (chosen by the operator or load need) to determine the present control's reference limit. Subtracting the actual current from the set reference limit generates an error signal which is transmitted to the proportional-integral (PI) controller in order to generate the desired angle order. The gamma control generates the inverter's gamma angle order using a second PI controller. The firing moment is found by comparing the two angle orders and taking the smaller of the two as the starting point for the calculation.

IV. ARTIFICIAL NEURAL NETWORKS

There have been many successes in creating intelligent systems, some of which were motivated by biological neural networks. Artificial neural networks are being designed by scientists from a wide range of fields to address issues in pattern recognition, prediction, optimization, associative memory, and control. For these issues, conventional methods have been presented as potential answers. Though there are applications that work effectively within narrow parameters, none of them can adapt to and thrive in uncharted territory. Exciting new options are provided by ANNs, and their use could be beneficial in many different contexts. If you're new to artificial neural networks and want to read the other papers in this issue of Computer, this article is for you.

Through millions of years of development, the human brain has acquired numerous useful properties that were not present in either Invon Neumann's original model or the most advanced parallel computers of today. The ability to learn and generalise, as well as the capacity for huge parallelism and distributed representation and processing, are examples of such features.

V. SIMULATION RESULTS

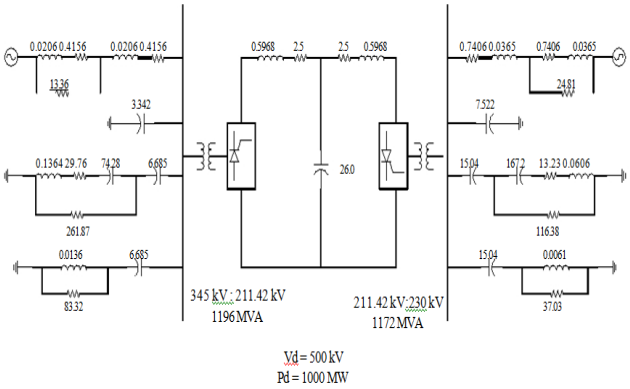

Figure 2. Schematic diagram of an HVDC transmission system

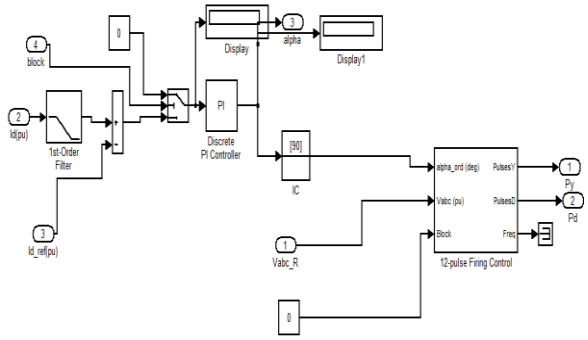

Figure 3. Rectifier control with PI.

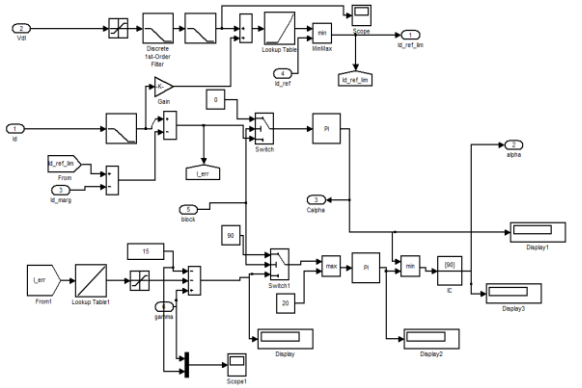

Figure 4. Inverter control with PI.

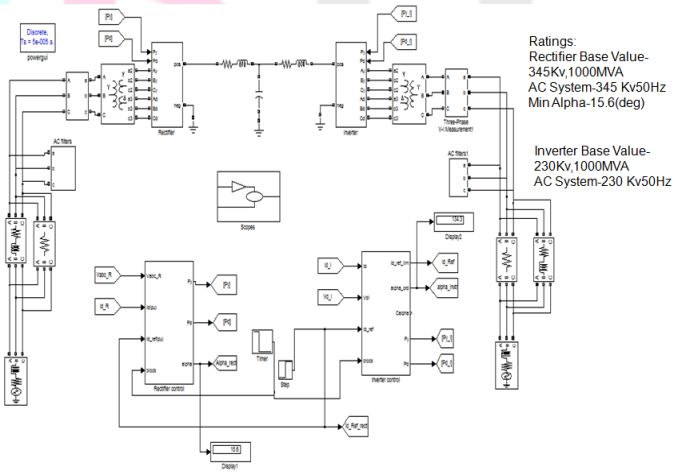

Figure 5. Simulink model of HVDC System

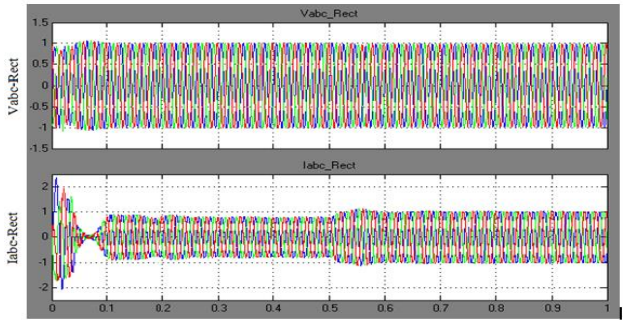

Figure 6. Rectifier side AC Voltage ad AC Current

In the preceding graph, the Rectifier AC side's three-phase voltage and current are shown in per units, indicating that they follow a sinusoidal pattern (p.u).

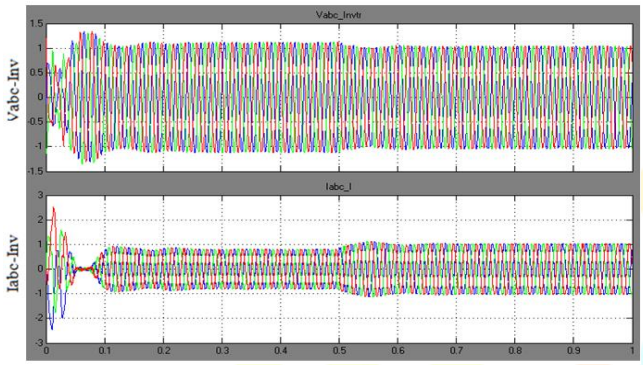

Figure 7. Inverter side AC Voltage ad AC Current

The preceding graph shows that the Inverter AC side's three-phase voltage and current are sinusoidal and expressed in pf (p.u).

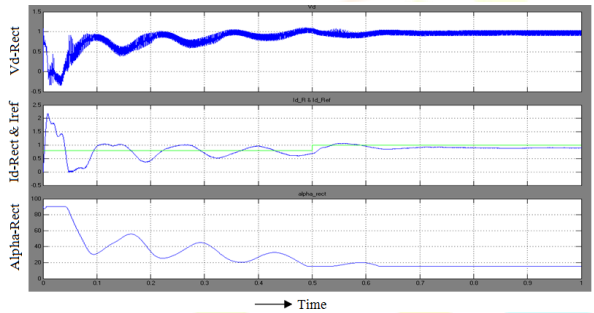

Figure 8. Rectifier side DC Voltage, DC Current and firing angle order with PI

The firing angle order (=15.5 deg) is obtained by comparing the values of Id R and Id Ref in the above graph via an error signal.

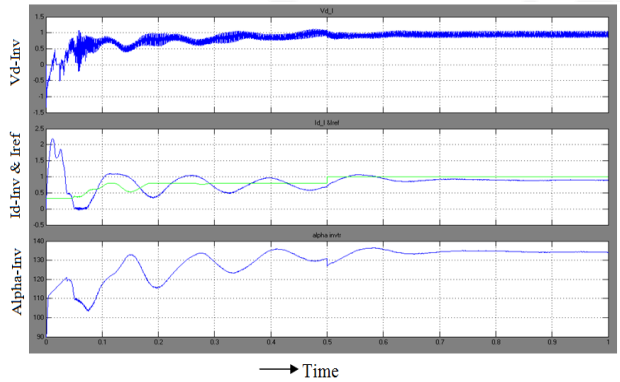

Figure 9. Inverter side DC Voltage, DC Current and firing angle order with PI

The firing angle order (=15.5 deg) is obtained by comparing the values of Id R and Id Ref in the above graph via an error signal.

Table 1. Effect due to change in Rectifier Firing Angle Using PI

Rectifier α (degrees)	Inverter α (degrees)	I_d_R (p.u)	I_d_I (p.u)	V_d_R (p.u)	V_d I (p.u)
15.5	134	0.8954	0.8913	1.016	0.8582
30	128.6	0.8496	0.844	0.83	0.840
45	119.4	0.6294	0.6261	0.749	0.6825
60	109.9	0.3848	0.3989	0.358	0.35
75	98.62	0.2469	0.2394	0.28	0.26

You can see from the table above that when the firing angle of the rectifier increases, the DC currents & DC voltages of the rectifier and inverter drop.

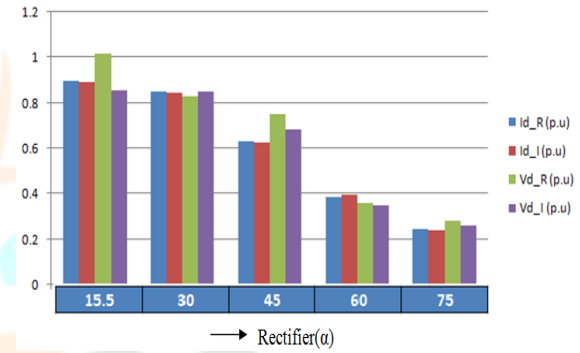

Figure 10. Effect due to change in Rectifier firing angle (chart representation) using PI

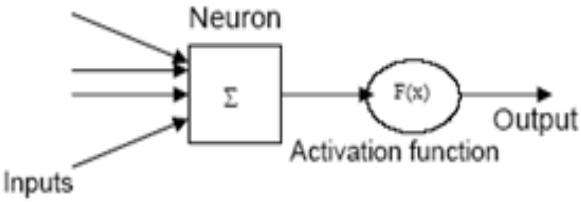

Figure 11. Simple Artificial Neuron

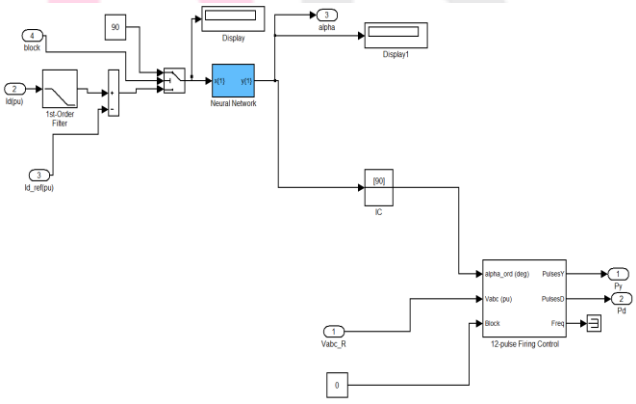

Figure 12. Rectifier control with Artificial Neural Network

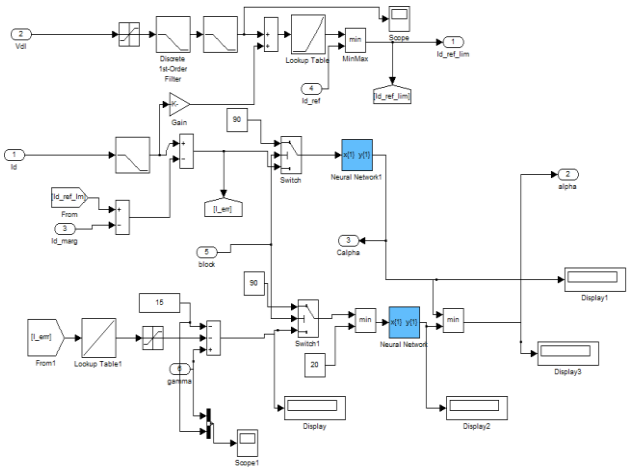

Figure 13. Inverter control with Artificial Neural Network

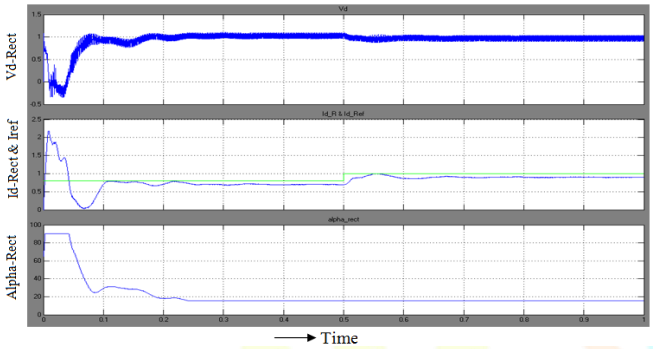

Figure 14. Rectifier side DC Voltage, DC Current and firing angle order with Artificial Neural Network

The firing angle order (=15.5 deg) is obtained by comparing the values of Id R and Id Ref in the above graph via an error signal.

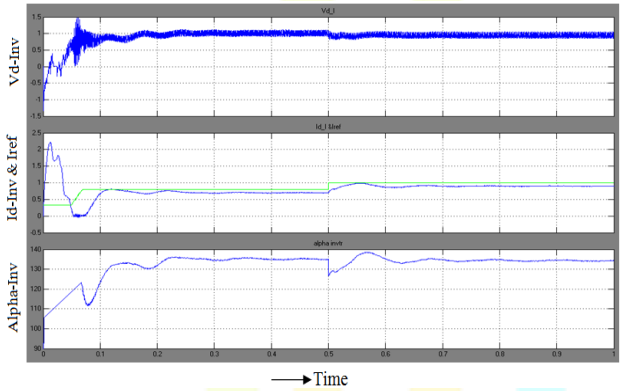

Figure 15. Inverter side DC Voltage, DC Current and firing angle order with Artificial Neural Network

The firing angle order (inv=142 deg) can be derived from the preceding graph by comparing Id I and Id Ref to generate an error signal.

Table 2. Effect due to change in Rectifier Firing Angle Using Artificial Neural Network

Rectifier α (degrees)	Inverter α (degrees)	I_d_R (p.u)	I_d_I (p.u)	V_d_R (p.u)	V_d I (p.u)
15.5	142	0.903	0.9024	1.019	0.869
30	1130	0.852	0.848	0.835	0.847
45	120.5	0.753	0.734	0.784	0.702
60	112	0.452	0.432	0.468	0.452
75	101	0.301	0.312	0.321	0.312

From the above table as the rectifier firing angle α increases, the DC currents and DC voltages of both rectifier and inverter are decreases.

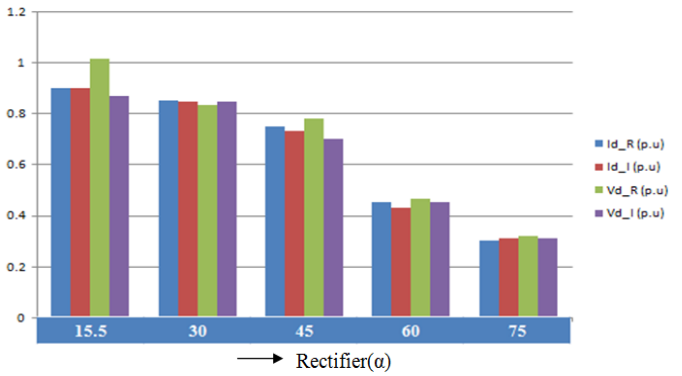

Figure 16. Effect due to change in Rectifier firing angle (chart representation) using ANN

TABLE 3. Comparison between PI and Artificial Neural Network for different Firing Angles

Rectifier α (deg)	Inverter α (deg)		Id_R (p.u)		Id_I (p.u)		Vd_R (p.u)		Vd_I (p.u)	
	PI	ANN	PI	ANN	PI	ANN	PI	ANN	PI	ANN
15.5	134.3	142	0.8954	0.9030	0.8990	0.9024	1.0160	1.0190	0.8587	0.8690
30	128.6	130	0.8496	0.8520	0.8440	0.8480	0.8300	0.8350	0.8400	0.8470
45	119.4	120.5	0.6294	0.7530	0.6261	0.7340	0.7490	0.7840	0.6825	0.7020
60	109.9	112	0.3848	0.4520	0.3989	0.4320	0.3580	0.4680	0.3500	0.4520
75	98.62	101	0.2469	0.3010	0.2394	0.3120	0.2800	0.3210	0.2600	0.3120

From the above table, the DC currents and voltages of both rectifier and inverter with Artificial Neural Network shows better values when compared with PI controller for different firing angles.

VI. CONCLUSION

In this research, we present an HVDC system that uses both a traditional controller and an Artificial Neural Network to regulate the current flowing between two converter stations. Control over current is employed in the rectifier, while current & extinction angle control are used in the inverter. When using a DC link, keeping the alpha to a minimum ensures the most power is sent. An error signal is fed into a controller comprised of PI & artificial neural networks, which then generates the appropriate firing angle order. This data is used by the firing circuit to provide evenly spaced pulses for the converter station's valves. This study compares the efficiency of a traditional controller with that of an Artificial Neural Network intended to control a rectifier and an inverter. As can be seen from the simulation results, the HVDC controlled by a neural network is far more adaptable than the conventional PI controller.

REFERENCES

[1]. M. O. Faruque, Yuyan Zhang and V. Dinavahi, "Detailed modeling of CIGRE HVDC benchmark system using PSCAD/EMTDC and PSB/SIMULINK," IEEE Trans. Power Delivery, vol.21, no.1, pp. 378 –387, Jan. 2006.

[2]. Das, B.P.; Watson, N.; Yonghe Liu; , "Simulation study of conventional and hybrid HVDC rectifier based on CIGRÉ benchmark model using PLL-less synchronisation scheme," Power Engineering and Optimization Conference (PEOCO), 2011 5th International , vol., no., pp.312-317, 6-7 June 2011doi: 10.1109/PEOCO.2011.5970433.

[3]. Ashfaq Thahir, M.; Kirthiga, M.V.; , "Investigations on modern self-defined controller for hybrid HVDC systems," TENCON 2011 - 2011 IEEE Region 10 Conference , vol., no., pp.938-943, 21-24 Nov. 2011doi: 10.1109/TENCON.2011.6129248.

[4]. Manoj, V. (2016). Sensorless Control of Induction Motor Based on Model Reference Adaptive System (MRAS). *International Journal For Research In Electronics & Electrical Engineering*, *2*(5), 01-06

[5]. V. B. Venkateswaran and V. Manoj, "State estimation of power system containing FACTS Controller and PMU," 2015 IEEE 9th International Conference on Intelligent Systems and Control (ISCO), 2015, pp. 1-6, doi: 10.1109/ISCO.2015.7282281.

[6]. Das, B.P.; Watson, N.; Yonghe Liu; , "Comparative study between gate firing units for CIGRE benchmark HVDC rectifier," Industrial Electronics and Applications (ICIEA), 2011 6th IEEE Conference on , vol.,no.,pp.299-306,21-23June2011 doi: 10.1109/ICIEA.2011.5975598.

[7]. Sood, V.K.; Khatri, V.; Jin, H.; , "EMTP modelling of CIGRE benchmark based HVDC transmission system operating with weak AC systems," Power Electronics, Drives and Energy Systems for Industrial Growth, 1996., Proceedings of the 1996 International Conference on , vol.1, no., pp.426-432 vol.1, 8-11 Jan 1996doi: 10.1109/PEDES.1996.539653.

[8]. Kala Meah, A.H.M. Sadrul Ula, "Simulation Study of the Frontier Line as a Multi-Terminal HVDC System," IEEE PES General Meeting, July 20- 24, 2008, Pittsburg, PA, USA.

[9]. N.G. Hingorani, "Power Electronics in Electronic Utilities: Role of Power Electronics in Future Power Systems," Proceeding of the IEEE, Vol. 76, No. 4, April, 1988, pp. 481-482.

[10]. Dinesh, L., Sesham, H., & Manoj, V. (2012, December). Simulation of D-Statcom with hysteresis current controller for harmonic reduction. In *2012 International Conference on Emerging Trends in Electrical Engineering and Energy Management (ICETEEEM)* (pp. 104-108). IEEE

[11]. Manohar, K., Durga, B., Manoj, V., & Chaitanya, D. K. (2011). Design Of Fuzzy Logic Controller In DC Link To Reduce Switching Losses In VSC Using MATLAB-SIMULINK. *Journal Of Research in Recent Trends*.

[12]. Manoj, V., Manohar, K., & Prasad, B. D. (2012). Reduction of switching losses in VSC using DC link fuzzy logic controller *Innovative Systems Design and Engineering ISSN*, 2222-1727

[13]. Dinesh, L., Harish, S., & Manoj, V. (2015). Simulation of UPQC-IG with adaptive neuro fuzzy controller (ANFIS) for power quality improvement. *Int J Electr Eng*, *10*, 249-268